



Original Article

## Efficiency Normal and Loaded Parthenolide on Nano-meso Particles as Antiproliferative Agent Against Breast Cancer Cell Line *In vitro*

Nesa Jafary<sup>1</sup>, Zohreh Rabiei<sup>1</sup>, Sattar Tahmasebi Enferadi<sup>1\*</sup>, Reza Behruzi<sup>1</sup> and Mario Scalet<sup>2</sup>

<sup>1</sup>National Institute of Genetic Engineering and Biotechnology (NIGEB), Shahrak-e- Pajooesh, 15th Km, Tehran - Karaj Highway, Tehran, Iran

<sup>2</sup>University of Udine, Department of Agricultural and Environmental Sciences, Udine, Italy

Article History: Received: 16 February 2019 /Accepted in revised form: 23 February 2019

© 2012 Iranian Society of Medicinal Plants. All rights reserve

### Abstract

Background: Parthenolide is major sesquiterpene lactones present in *Tanacetum parthenium* (L.) Sch.Bip. (feverfew). This compound is known as herbal active principals with potential use in pharmaceutical and medicine. In order to solubility improving, analogue of Parthenolide, aminopropyl theoxy silane -mesoporous silica of Parthenolide, was synthesized as well. In this study, it was extracted from fresh flowers of feverfew and was purified and identified by chromatography methods Cell death of breast cancer cell line MDA-MB-231 was assayed 24 hour after administration of normal and nanoparticle Parthenolide by Methylthiazol Tetrazolium test and Annexin-V-Fluorescein kit and scanning electron microscopy. The results revealed that anti-growth effect of Parthenolide is independent of exposure time and induced apoptosis in cancer cells yet this effect on fibroblast cells as normal ones did not recognized which guarantees the use of this medicinal herb to treat cancers without promotion of other not interested side effect.

**Keywords:** Cell viability; HPLC; mesoporous silica of PTL; parthenolide; MTT test

**Abbreviation:** **APTES-MS-PFPTL:** Purified feverfew flower ParThenoLide loaded on AminoPropyl ThEoxySilane-Mesoporous Silica; **FPTL:** Feverfew Flower extract containing ParThenoLide; **MTT:** Methylthiazol Tetrazolium; **PFPTL:** Purified feverfew Flower ParThenoLide; **PTL:** ParThenoLide

### Introduction

Parthenolide (PTL) is the main extracts of sesquiterpene lactone, a class of plant secondary metabolites with over 4000 known structures, isolated from *Tanacetum parthenium* (L.) Sch.Bip. (feverfew) and is reported to be the main bioactive compound with several functions in feverfew inducing inhibition of proliferation and apoptosis in various human cancer cells [1, 2]. Feverfew formerly *Chrysanthemum parthenium* (L.) Pers. has been used

for medicinal purposes to treat dermatitis, inflammation, migraine, menstrual, irregularities, fever, rheumatoid arthritis and mouth ulcers since the middle ages [1,3]. PTL has been predominately investigated as an anticancer agent numerous cancer types, both *in vitro* and *in vivo*. Specifically, PTL has been tested against cervical cancer [4], glioblastoma [5], breast cancer [6, 7], leukemia [8-10], Pancreatic cancer [11], prostat cancer [12, 13], lung cancer [4], melanomas [14,15] and colon cancer [16].

\*Corresponding author: National Institute of Genetic Engineering and Biotechnology (NIGEB), Shahrak-e- Pajooesh, 15th Km, Tehran -Karaj Highway, Tehran, Iran  
Email Address: tahmasebi@nigeb.ac.ir

PTL can sensitize resistant cancer cells to antitumor agents [17], and act as a chemo-preventive agent in an animal model of UVB-induced (ultraviolet radiation B, 290-320 nm) skin cancer [18]. It is assumed to be linked with either antitumor effect due to making changes at the DNA replication level or the suppression of T-cells from activation-induced cell death [19]. Meanwhile data have showed that PTL-induced apoptosis is associated with inhibition of transcription factor nuclear factor-kappa B (NF-kB) [20, 21]. Mitochondrial dysfunction and increase of reactive oxygen [2, 6, 16, 22]. However the detailed molecular mechanisms of anticancer effect of PTL are largely unknown [23-25] and is expected to be affected by the quantity of PTL and its exposure time with cancer cells. Apoptotic induction has been a new target mechanism for novel drug discovery. Bax and p53 is well known to be an important upstream effector molecule in the apoptotic pathway as a potent inducer of apoptosis [25].

Breast cancer is the most common cancer worldwide that affecting women with high prevalence in developed countries so that over one million new cases reported each year. A current approach for breast carcinoma chemotherapy is use of pharmaceutical agents with inducing death of breast tumor property. So finding apoptotic inducer from plant either frees or compound form is important.

It is reported that a concentration of  $2.3 \mu\text{g}\cdot\text{mL}^{-1}$  of PTL had cytotoxic activity against the human epidermoid carcinoma [19, 26].

It has been reported that some sesquiterpene lactones can conjugate with intracellular thiols and induce apoptosis [16]. Apoptosis, a programmed cell death which is important in controlling cell number and proliferation induces by two major pathways; extrinsic and intrinsic pathways. Evading apoptosis is one of the hallmark of cancer cells [27]. PTL induces apoptosis through different mechanism of them activation of reactive oxygen species (ROS) as a mediated molecule to induce apoptosis via intrinsic apoptotic signaling pathway [2, 28]. PTL contributes the extrinsic apoptosis through inhibition of NF-kB, STATs transcriptional activity, and resulting down-regulation of related genes [29]. PTL effects against different cancer cell lines by altering experience genes under NF-KB control, but PTL has poor water solubility as well [1,30,31].

Although recent research examined the efficacy of PTL *in vivo* pointing out its insufficient bioavailability as PTL has poor solubility and high reactivity with serum which limits its *in vivo* use [31]. As an alternative approach to improve PTL solubility, its analogues have been synthesized by nanoparticle. Cyclopropyl analogue, PTL GSH and PTL cysteine conjugates have higher  $\text{IC}_{50}$  (half maximal inhibitory concentration) value compared with free PTL [1].

In the present research, to corroborate the efficiency of PTL on growth inhibition of MDA-MB-231 cell line, we evaluated the impact of *in vitro* treatment of both normal and aminopropyl theoxy silane - mesoporous silica of PTL on MDA-MB-231 breast cancer cell line which does not express oestrogene, progesteron and ER-2-neu receptors. The examined breast cancer cell line is unresponsive to trastuzumab and must be treated with several other therapies for example surgery, radiation therapy and chemotherapy [32].

#### Objectives

To extract and purify PTL originated fresh feverfew's flowers and to assess the potential anti-proliferation of nanoparticle and normal PTL on breast cancer cell line *in vitro*.

#### Material and Methods

##### Parthenolide (PTL) extraction and purification

*Thanaacetum parthenium* (L.) Sch.Bip. plants were collected from Hamadan province (34.7982 °N, 48.5146 ° E), Iran and were identified and registered by deposit number 006420 in herbarium of Tehran university. Extraction of PTL was performed by Majdi methods from flower, leave and stem [33].

##### 3-2- PTL identification: HPLC and FT-IR

PTL presence was confirmed through HPLC analysis comparing with PTL standard solution. PTL was quantified by using standard curve. Since the higher amount of extracted PTL was obtained from the flower extract, we conducted the rest of the analysis on feverfew flower extract containing PTL (FPTL). HPLC analysis was performed for effectively purification of PTL using Cecil 1100 series (Cecil Inst., Ltd Cambridge, United Kingdom) equipped

with a 1100 series pump and UV absorbance detector, a column oven (CTS-30 Yanglin, Korea) and a Octadecylsilane (ODS), C18 column. The mobile phase consisted of ultra-pure water and acetonitrile with a flow rate of  $1.5 \text{ ml}\cdot\text{min}^{-1}$  at room temperature ( $25 \text{ }^\circ\text{C}$ ). An authentic standard of PTL (Sigma, USA) was prepared at four concentrations (50-100-200-400 ppm) in methanol and was used to make the calibration curve. Flower extract further was purified by Colum chromatography with n-Hexane/Benzane/Acetonitrile (30:21:15 v/v) as mobile phase [32]. 15 fractions were obtained by this method, and then purified fraction was diagnosed via HPLC analysis. Both FPTL and purified PTL feverfew flower extract (PFPTL) were dissolved in ethanol.

Fourier Transformation-Infrared Spectroscopy (FT-IR) spectra were recorded on FT-IR spectrophotometer (BRUKER, Germany) using KBr discs. The PTL ( $2 \mu\text{l}$ ) was coated on the KBr discs to form thin liquid films for infrared spectrometry analysis. The discs were approximately 5 mm in diameter and 1 mm in thickness. The instrument was operated under dry air purge, and the scans were collected at scanning speed of  $2 \text{ mm}\cdot\text{s}^{-1}$  with resolution of  $4 \text{ cm}^{-1}$  over the region of  $4000\text{--}400 \text{ cm}^{-1}$ .

#### Synthesis of Parthenolide analogue; Aminopropyl Theoxy Silane -Mesoporous Silica of Parthenolide (APTES-MS-PFPTL)

The amount of 500 g silica nano-particles was dissolved in ethanol (50 ml) and was treated with ultrasonic waves for 15 min. After adjusting pH at 3.5-4, aminopropyl Theoxy Silane (500 mg) was added and the reaction continued for 3 h while stirred at 28 g and further 5 min at 5000 g. This solution, called APTES-MS, was left overnight at  $20 \text{ }^\circ\text{C}$ . Consequently, 10 mg of PFPTL were separately dissolved in ethanol and then added to 10 ml of APTES-MS and were centrifuged at 1000 g for 5 min. The pellet was washed out with ethanol and supernatant was collected which included APTES-MS-PFPTL. To evaluate the real state of APTES-MS-PFPTL, the absorbance of solutions was read at 214 nm.

The analysis to evaluate anti-growth activity of APTES-MS-PFPTL at different concentration of PFPTL (0.5, 1, 1.5, 2, 2.5, 5, 10  $\mu\text{M}$ ) was assessed on MDA-MB-231 cell line.

#### Cell Line Anti-growth Activity Assay

MDA-MB-231 cells were maintained in DMEM medium with 100 U.ml<sup>-1</sup> of penicillin,  $100 \mu\text{g}\cdot\text{ml}^{-1}$  of streptomycin, and 10% fetal bovine serum (FBS). During the analysis to evaluate anti-growth activity of PTL on cell line, the cells were maintained in a humidified, 5%  $\text{CO}_2$  incubator at  $37^\circ\text{C}$  in the presence of different concentration of FPTL (60, 125, 175, 250, 300, 600, 1250 and  $2500 \mu\text{g}\cdot\text{ml}^{-1}$ ) and PFPTL (0.5, 1, 1.5, 2, 2.5, 5, 10 and  $20 \mu\text{M}$ ).

Methylthiazol Tetrazolium (MTT) assay was used to investigate anti-growth effects of both FPTL and PFPTL on MDA-MB-231 breast cancer cell line. The absorbance of treated and control cells were read by ELISA plate reader at 590-630 nm.

#### Analysis of Cell Death with Annexin-V-Flouos kit

Cells were treated with FPTL and PFPTL extracts at the indicated concentration (half maximal inhibitory concentration,  $\text{IC}_{50}$ ) for 24h. The detection of apoptotic or necrotic cells was carried out by dual staining with FITC conjugated to Annexin and PI (Roch Diagnostics, Mannheim, Germany).

#### Statistical Analysis

Statistical analysis was performed using the SPSS (Statistical Package for Social Sciences) software. T-test was used for finding significant differences. Differences with P values  $< 0.001$  were considered as significant.

## Result

#### Parthenolide Purification and Identification

Fifteen fractions were collected by column chromatography and finally one fraction as pure fraction was separated. The percentage of PTL peak area was calculated 7% of total peak area (Fig.1 A).

#### 4-2- Synthesis analogue of PTL with nanoparticle

Mesoporus silica nano-particles of aminopropyl theoxysilane (APTES-MS) and its combination with extracted PTL have prepared (APTES-MS-PFPTL). The schematic of aminopropyl theoxysilane-mesoporous silica preparation and the chemical structure of PTL are shown in chemical structure 1A and 1B.

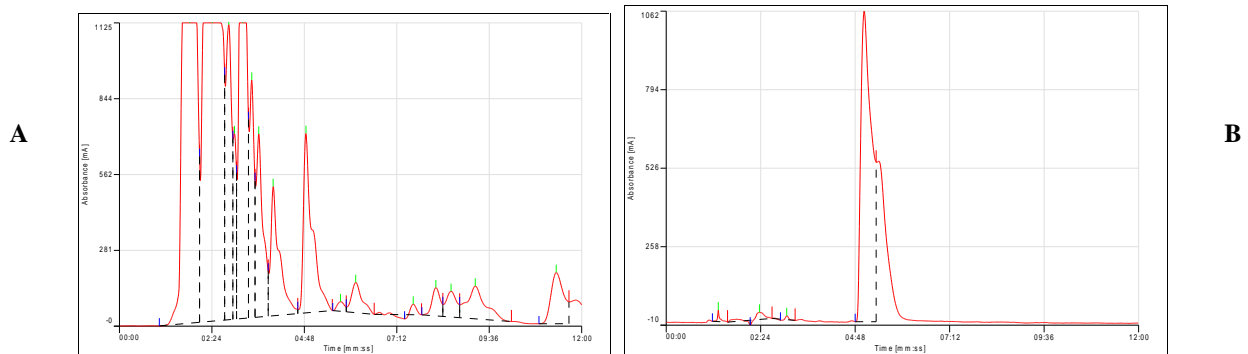
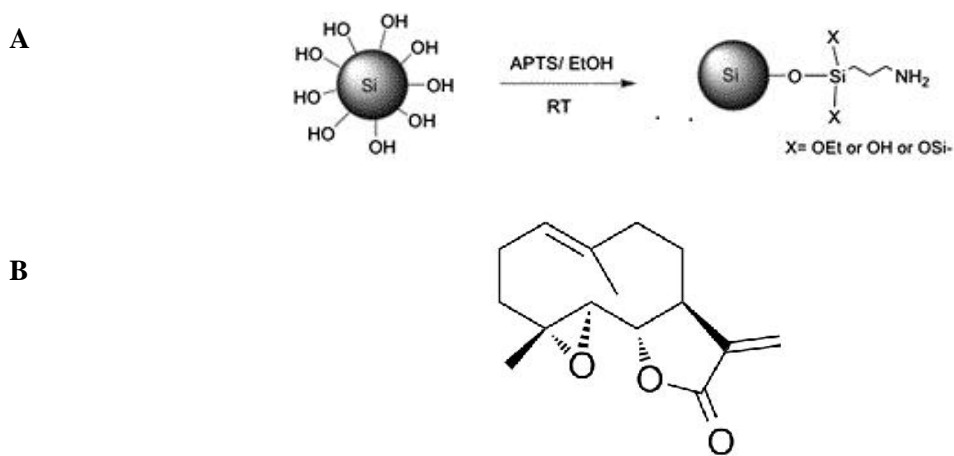


**Fig. 1** HPLC chromatogram of A) FPTL B) PFPTL. The arrow shows the peak of PTL



**Chemical structure 1** A) Preparation of APTES-MS B) the chemical structure of PTL

**Fig. 2** demonstrates the absorbance of PTL, APTES-MS-PFPTL and APTES-MS at 214 nm with FT-IR at frequency regions 4000-400  $\text{cm}^{-1}$ .

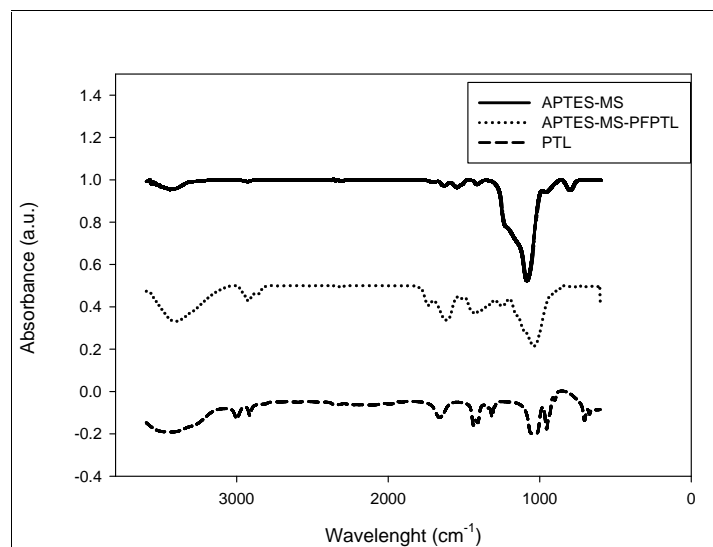
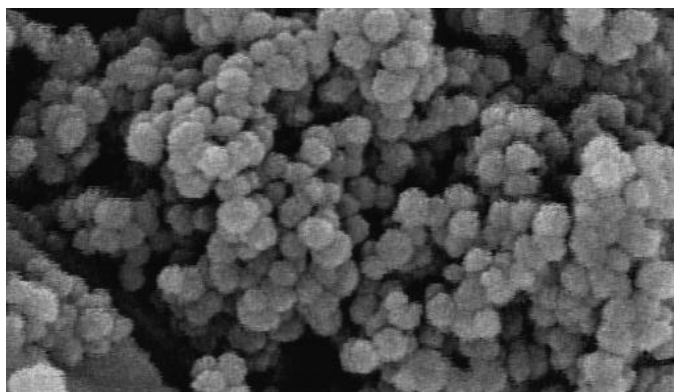


**Fig. 2** FT-IR spectrum of mesoporous silica nanoparticle with APTES-MS, APTES-MS-PFPTL and PTL.

The details of distinguished peaks representative for different chemical groups or bonds related to the wavelengths are summarized in the Table 1. As shown in Fig. 3 the Nano-structure of APTES-MS visualized by SEM. The efficiency of PTL loading on APTES was 95%.

**Table 1.** Different chemical groups or bonds related to the wavelengths, for A) APTES-MS, B) APTES-MS-PFPTL, C) PFPTL

<b>A</b>	
<b>Wavelength</b>	<b>group</b>
1000-1100	C—O
3500	OH
<b>B</b>	
<b>Wavelength</b>	<b>group</b>
1000-1100	C—O Epoxy group
1300-1500	Flexural vibration of CH <sub>2</sub> , CH <sub>3</sub>
1715	C=O
3000	Stretching vibrations of CH <sub>2</sub> , CH <sub>3</sub>
3500	NH Functional group
<b>C</b>	
<b>Wavelength</b>	<b>Group</b>
1000-1100	C—O Epoxy group
1300-1500	Flexural vibration of CH <sub>2</sub> , CH <sub>3</sub>
1715	C=O
3000	Stretching vibrations of CH <sub>2</sub> , CH <sub>3</sub> and =CH <sub>2</sub>
3500	OH



500 nm

**Fig. 3** APTES-MS nanoparticle visualized by scanning electron microscopy (SEM)

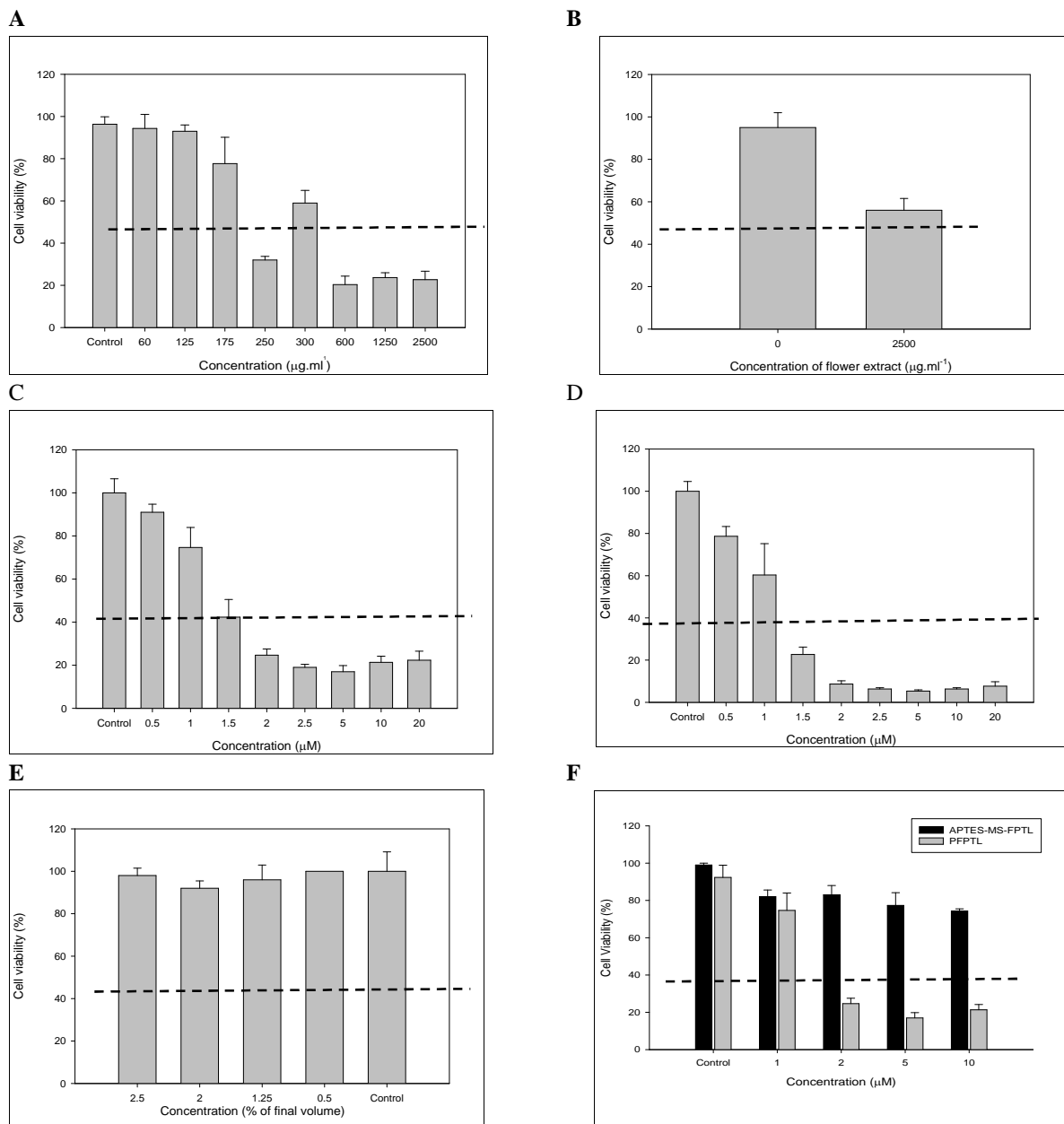


**Fig. 4** Cell viability (%) assigned by MTT assay of A) FPTL, exposed on MDA-MB-231 cancer cell line for 24 h, B) FPTL exposure on fibroblast cells, C) PFPTL, exposed on MDA-MB-231 cancer cell line for 24 h, D) PFPTL exposed on MDA-MB-231 cancer cell line for 48 h, E) equivalent concentration of ethanol as vehicle, F) APTES-MS-PFPTL, and extracted PTL exposed on MDA-MB-231 cancer cell line for 24 h. Dash lines shows  $\text{IC}_{50}$  threshold

#### Microscopic Identification of Cells Treated with FPTL

The morphological changes occurred due to FPTL treatment on cell line MDA-MB-231 at  $600 \mu\text{g.ml}^{-1}$  for 24 h has investigated through optical microscope

(Fig. 5). Indeed, the effect of  $600 \mu\text{g.ml}^{-1}$  FPTL for 24 h on the studied cell line was followed by scanning electron microscopy (SEM) (Fig. 6).

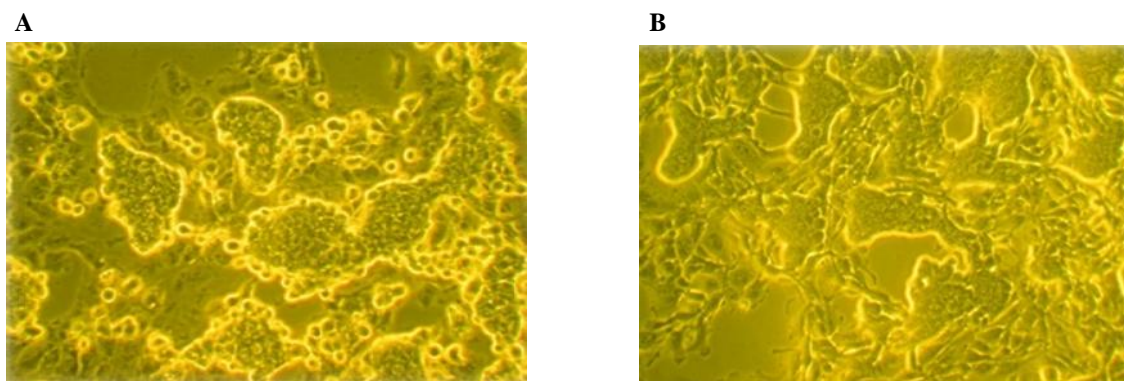


**Fig. 5** Cell morphology of MDA-MB231 treated with  $600 \mu\text{g}\cdot\text{ml}^{-1}$  FPTL, for 24h. Optical microscopy, 100X. A) Treated cells, B) control.

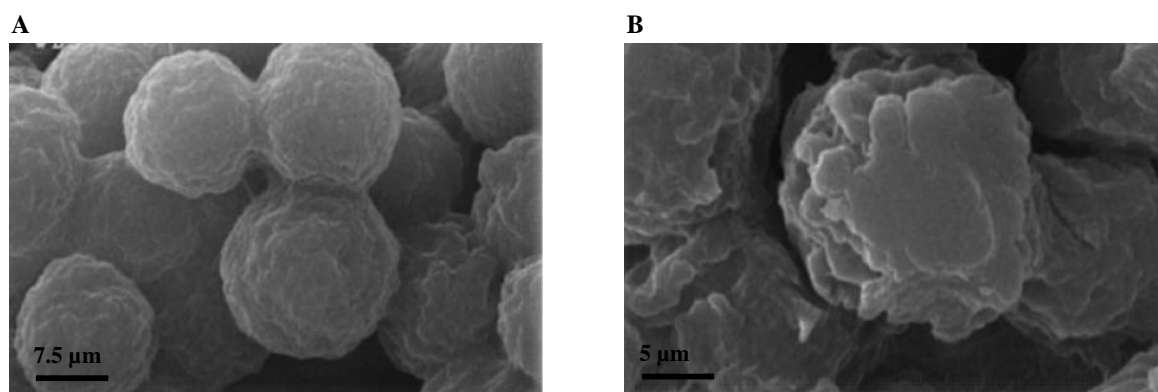


**Fig. 6** Morphological changes of MDA-MB-231 treated with  $600 \mu\text{g}\cdot\text{ml}^{-1}$  FPTL visualized by scanning electron microscopy (SEM). A) control, B) treated cells

## Discussion

PTL was extracted from different parts (flower, leave, and stem) of feverfew. However, the significant amount of PTL was only obtained from feverfew's flowers with methanol and formic acid. The column chromatography purified extract analyzed by HPLC provided PTL peak equivalent to  $33 \text{ mg}\cdot 100\text{g}^{-1}$  in feverfew's flower (Fig. 1B).

As shown in Table the same functional groups were distinguished for both APTES-MS-PFPTL and PFPTL including wavelengths 1000-1100, 1300-1500, 1715, 3000 representing C=O epoxy group, flexural vibration of CH<sub>2</sub> and CH<sub>3</sub>, C=O and stretching vibration of CH<sub>2</sub> and CH<sub>3</sub>, respectively. The only wavelength (3500) with different functional group (OH) refers to nanoparticle construction which confirmed accordingly FT-IR of APTES-MS.

The results of proliferation inhibitory rate analysis (figure 4A-D) confirmed that the higher concentration of the extracted PTL, the more potential in cell growth suppression. Although the time of exposure has proved to not be a crucial parameter rate as IC<sub>50</sub> remained constant for both 24 h and 48 h exposure time, Considering  $600 \mu\text{g}\cdot\text{ml}^{-1}$  and  $1.5\mu\text{M}$  of the extract as IC<sub>50</sub> for FPTL and PFPTL, respectively. Researchers reported that PTL displayed potent anticancer effects and induced cell death but in a concentration less than other report [1]. According figure 4B even though at the most concentrated FPTL ( $2500 \mu\text{g}\cdot\text{ml}^{-1}$ ) induced inhibition in proliferation, the cell viability (%) was higher than IC<sub>50</sub> for FPTL, which confirms the non-toxicity effect of PTL on normal cells. However figure 4F provides data on the inhibition of APTES-MS-PFPTL on MDA-MB-231 cancer cell line proliferation compared with PFPTL. Studies suggest that some analogue of PTL such as DMAPT can be a candidate

for triple-negative breast cancers (TNBCs) therapy [32]. Here loading PTL on APTES-MS nanoparticle improved water solubility but couldn't induce cell death with apoptosis. Improving the cytotoxic activity of PTL on breast cancer need to another strategy such as its combination with other compound [6, 32].

The cell morphology of MDA-MB-231 treated with 600  $\mu\text{g}\cdot\text{ml}^{-1}$  of FPTL confirmed apoptosis mode of cell death according to microscopic inspection (figure 5). Other studied demonstrated that 25  $\mu\text{M}$  PTL could stimulate ROS generation cell death by necrosis and autophagy [32]. Other showed that the PTL activates both apoptosis pathway and AMPK-autophagy survival pathway through the generation of ROS [1]. Although, the positive impact of PTL (in the forms of purified or mesoporous nanoparticle) originated feverfew has proven in this study, its suggested to follow up the same treatment *in vivo* as the bioavailability of such macro molecules obeys several physicochemical rules which are not simulatable in the *in vitro* analysis.

## References

- Lu C, Wang W, Jia Y, Liu X, Tong Z, Li B. Inhibition of AMPK/Autophagy Potentiates Parthenolide-Induced Apoptosis in Human Breast Cancer Cells. *J C biochem.* 2014;115:1458-1470.
- Wang W, Adachi M, Kawamura R, Sakamoto H, Hayashi T, Ishida T, Imai K., Shinomura Y. Parthenolide-induced apoptosis in multiple myeloma cells involves reactive oxygen species generation and cell sensitivity depends on catalase activity. *Apop.* 2006;11:2225-2240.
- Czyz M, Lesiak-Mieczkowska K, Koprowska K, Szulawska-Mroczek A, Wozniak M. Cell context-dependent activities of parthenolide in primary and metastatic melanoma cells. *Brit J pharma.* 2010;160:1144-1160.
- Jin X, Qiu L, Zhang D, Zhang M, Wang Z, Guo Z, Deng C, Guo C. Chemosensitization in non-small cell lung cancer cells by IKK inhibitor occurs via NF- $\kappa$ B and mitochondrial cytochrome c cascade. *J cell and mol med.* 2009;13:4596-4610.
- Anderson JC, Farland BC, Gladson CL. New molecular targets in angiogenic vessels of glioblastoma tumours. *Exp Rev Mol Med.* 2008;10:23-40.
- Nakshatri H, Rice SE, Bhat-Nakshatri P. Antitumor agent parthenolide reverses resistance of breast cancer cells to tumor necrosis factor-related apoptosis-inducing ligand through sustained activation of c-Jun N-terminal kinase. *Oncol.* 2004;23:7330-7350.
- Sweeney CJ, Mehrotra S, Sadaria MR, Kumar S, Shortle NH, Roman Y, Sheridan C, Campbell RA, Murry DJ, Badve S. The sesquiterpene lactone parthenolide in combination with docetaxel reduces metastasis and improves survival in a xenograft model of breast cancer. *Mol can ther.* 2005;4:1004-1020.
- Guzman M L, Rossi R M, Karnischky L, Li X, Peterson D R, Howard D S, Jordan C T. The sesquiterpene lactone parthenolide induces apoptosis of human acute myelogenous leukemia stem and progenitor cells. *Blood.* 2005;105:4163-4180.
- Neelakantan S, Nasim S, Guzman M L, Jordan C T, Crooks P A. Amino parthenolides as novel anti-leukemic agents: Discovery of the NF- $\kappa$ B inhibitor, DMAPT (LC-1). *Bio & med chem lett.* 2009;19:4346-4360.
- Hewamana S, Alghazal S, Lin T, Clement M, Jenkins C, Guzman M L, Jordan C T, Neelakantan S, Crooks P A, Burnett A K. The NF- $\kappa$ B subunit Rel A is associated with *in vitro* survival and clinical disease progression in chronic lymphocytic leukemia and represents a promising therapeutic target. *Blood.* 2008;111:4681-4700.
- Ramachandran C, Resek A P, Escalon E, Aviram A, Melnick S J. Potentiation of gemcitabine by Turmeric Force™ in pancreatic cancer cell lines. *Oncol Rep.* 2010;23:1529-1540.
- Shanmugam R, Jayaprakasan V, Gokmen-Polar Y, Kelich S, Miller K.D, Yip-Schneider M, Cheng L, Bhat-Nakshatri P, Sledge GW, Nakshatri H. Restoring chemotherapy and hormone therapy sensitivity by parthenolide in a xenograft hormone refractory prostate cancer model. *The Prost.* 2006;66:1498 -1510.
- Sweeney C, Li L, Shanmugam R, Bhat-Nakshatri P, Jayaprakasan V, Baldrige L A, Gardner T, Smith M, Nakshatri H, Cheng L. Nuclear factor- $\kappa$ B is constitutively activated in prostate cancer *in vitro* and is overexpressed in prostatic intraepithelial neoplasia and adenocarcinoma of the prostate. *Clin Can Res.* 2004; 10: 5501-5520.
- Kim K W, Cho M L, Kim H R, Ju J H, Park M K Oh H J, Kim J S, Park S H, Lee S H, Kim H Y. Up-regulation of stromal cell-derived factor 1 (CXCL12) production in rheumatoid synovial fibroblasts through interactions with T lymphocytes: Role of interleukin-17 and CD40L-CD40 interaction. *Arth & Rheu.* 2007;56:1076-1090.
- Suvannasankha A, Crean C D, Shanmugam R, Farag S S, Abonour R, Boswell H S, Nakshatri H. Antimyeloma effects of a sesquiterpene lactone parthenolide. *Clin Can Res.* 2008;14:1814-1830.
- Zhang S, Ong CN, Shen HM. Critical roles of intracellular thiols and calcium in parthenolide-induced apoptosis in human colorectal cancer cells. *Can Let.* 2004; 208:143-154.
- Parada-Turska J, Paduch R, Majdan M, Kandeferszewska M, Rzeski W. Antiproliferative activity of parthenolide against three human cancer cell lines and

- human umbilical vein endothelial cells. *Pharm Rep.* 2007; 59:233-245.
18. Koprowska K, Czy M, Nowotworów Z B M. Molekularne mechanizmy działania parthenolidu—stary lek z nową twarzą. Molecular mechanisms of parthenolide action: Old drug with a new face. *J Cover.* 2015;69:75-85.
  19. Wu C, Chen F, Rushing J W, Wang X, Kim H J, Huang G, Haley-Zitlin V, He G. Antiproliferative activities of parthenolide and golden feverfew extract against three human cancer cell lines. *J Med Food.* 2006;9:55-70.
  20. Sahler J, Bernard J J, Spinelli S L, Blumberg N, Phipps R P. The Feverfew plant-derived compound, parthenolide enhances platelet production and attenuates platelet activation through NF- $\kappa$ B inhibition. *Thromb Res.* 2011;127:426-440.
  21. Won Y K, Ong C N, Shi X, Shen H M. Chemopreventive activity of parthenolide against UVB-induced skin cancer and its mechanisms. *Carcino.* 2004; 25:1449-1460.
  22. Cheng G, Xie L. Parthenolide induces apoptosis and cell cycle arrest of human 5637 bladder cancer cells *in vitro*. *Mol.* 2011;16:6758-6765.
  23. Cijo George V, Kumar DN, Suresh P, Kumar RA. A review on the therapeutic potentials of parthenolide: A sesquiterpene lactone. *Int Res J Pharm.* 2012;3:69-80.
  24. Zhao X, Liu X, Su L. Parthenolide induces apoptosis via TNFRSF10B and PMAIP1 pathways in human lung cancer cells. *J Exp & Clin Can Res.* 2014;33:1-9.
  25. Liu J W, Cai M X, Xin Y, Wu Q S, Ma J, Yang P, Xie H Y, Huang D S. Parthenolide induces proliferation inhibition and apoptosis of pancreatic cancer cells *in vitro*. *J Exp & Clin Can Res.* 2010;29:1-10.
  26. Ghantous A, Gali-Muhtasib H, Vuorela H, Saliba N A, Darwiche N. What made sesquiterpene lactones reach cancer clinical trials?. *Drug disc today.* 2010;15:668-674.
  27. Shabani S H S, Tehrani S S H, Rabiei Z, Enferadi S T, Vannozzi G P. *Peganum harmala* L.'s anti-growth effect on a breast cancer cell line. *Biotech Rep.* 2015;8:138-145.
  28. Mathema V B, Koh Y-S, Thakuri B C, Sillanpää M. Parthenolide, a sesquiterpene lactone, expresses multiple anti-cancer and anti-inflammatory activities. *Inflam.* 2012;35:560-570.
  29. Kim I H, Kim S W, Kim S H, Lee S O, Lee S T, Kim D-G, Lee M-J, Park W H. Parthenolide-induced apoptosis of hepatic stellate cells and anti-fibrotic effects in an *in vivo* rat model. *Expe & mole med.* 2012;44:448-460.
  30. Weng S, Sui M, Chen S, Wang J-a, Xu G, Ma J, Shan J, Fang L. Parthenolide inhibits proliferation of vascular smooth muscle cells through induction of G0/G1 phase cell cycle arrest. *J Zhej Uni Sci.* 2009;10:528-540.
  31. Zong H, Sen S, Zhang G, Albayati C Mu, Gorenstein Z D, Liu X, Ferrari M, Crooks P, Roboz G. *In vivo* targeting of leukemia stem cells by directing parthenolide-loaded nanoparticles to the bone marrow niche. *Leuke.* 2015;4:143-153.
  32. D'Anneo A, Carlisi D, Lauricella M, Puleio R, Martinez R, Di Bella S, Di Marco P, Emanuele S, Di Fiore R, Guercio A. Parthenolide generates reactive oxygen species and autophagy in MDA-MB231 cells. A soluble parthenolide analogue inhibits tumour growth and metastasis in a xenograft model of breast cancer. *Cell Death & Dis.* 2013;4:891-910.
  33. Majdi M, Liu Q, Karimzadeh G, Malboobi MA, Beekwilder J, Cankar K, de Vos R, Todorovi S, Simonovi A, Bouwmeester H. Biosynthesis and localization of parthenolide in glandular trichomes of feverfew (*Tanacetum parthenium* L. Schulz Bip.). *Phyto.* 2011;72:1739-1750.